Rotational Doppler shift of a phase-conjugated photon

A. Yu. Okulov

Russian Academy of Sciences, Moscow, Russia (alexey.okulov@gmail.com)

Received September 27, 2011; revised December 12, 2011; accepted December 29, 2011;
posted January 6, 2012 (Doc. ID 155277); published March 20, 2012

The rotational Doppler shift of a photon with orbital angular momentum $\pm\ell\hbar$ is shown to be an even multiple of the angular frequency Ω of the reference frame rotation when the photon is reflected from the phase-conjugating mirror. The one-arm phase-conjugating interferometer is considered. It contains N Dove prisms or other angular-momentum-altering elements rotating in opposite directions. When such interferometer is placed in the rotating vehicle, the $\delta\omega = 4(N + 1/2)\ell \cdot \Omega$ rotational Doppler shift appears. As a result, the helical interference pattern will rotate with angular frequency $\delta\omega/2\ell$. The accumulation of angular Doppler shift via successive passages through the N image-inverting prisms is due to the phase conjugation; for a conventional parabolic retroreflector, the accumulation is absent. The features of such a vortex phase-conjugating interferometry at the single-photon level are discussed.

OCIS codes: 020.7010, 030.6140, 050.4865, 070.5040, 140.3560, 160.1585.

1. INTRODUCTION

Single-photon interferometry utilizes the superposition of mutually coherent quantum states Ψ_j [1] to which a photon belongs simultaneously. The interference pattern depends on a method of Ψ_j preparation. A double-slit Young interferometer creates two free-space wave functions, Ψ_1 and Ψ_2, whose interference pattern, produced by detection of the individual photons, is recorded by an array of detectors or a photographic plate located in the near or far field. In a Mach–Zehnder configuration [2,3], two wave functions separated by an entrance beam splitter recombine at the output beam splitter. The Michelson interferometer recombines at the input beam splitter two *retroflected* quantum states, provided these states are phase locked and their path difference δL is smaller than the coherence length L_c. Thus, the interference pattern is simply $\sim[1 + V(\delta L) \cdot \cos(k \cdot \delta L)]$, where $V(\delta L)$ is a visibility or second-order correlation function and $k = 2\pi/\lambda$. When retroreflection is accompanied by wavefront reversal realized with phase-conjugating mirrors (PCMs) [4] based upon stimulated Brillouin scattering [5,6], photorefractivity [7,8], or holographic PCMs, the optical path δL difference is almost entirely compensated due to phase conjugation (PC). Noteworthy is the observable phase lag via the relatively small frequency shift $\delta\omega = \omega_f - \omega_b$ arising due to the excitation of internal waves inside the PCM volume [9], where ω_f and ω_b are the carrier frequencies of incident and PC-reflected photons, respectively. This leads to the *frequency shift modulated* interference term $1 + V(\delta L) \cdot \cos(\delta k \cdot \delta L)$, where $\delta k = \delta\omega/c$ [6].

The aim of this article is to present the other nontrivial property of the phase-conjugated optical vortex fields and their single photons. The predicted effect is in the accumulation of the small Doppler frequency shifts [3,10–14] caused by very slow rotations of the phase-conjugated interferometer as a whole and the optical components therein. This effect takes place for the photon in the optical vortex quantum state [2,3] with topological charge ℓ, where the angular momentum $L_z = \pm\ell \cdot \hbar$ [15] is due to the phase singularity located at propagation axis z. Hereafter, the spin component of angular momentum [16] is supposed to be zero due to the linear polarization. It is convenient to use the single-photon wave functions that coincide with the positive frequency component of the electric field envelope $|\Psi\rangle = \sqrt{2\epsilon_0} \cdot E(t, \vec{r})$ [17]. The square modulus of Ψ is proportional to the energy density of the *continuous wave* (CW) laser beams and to the photon count rate in different fringes of the interference pattern for the single-photon experiments [18]. We will assume that Ψ is a Laguerre–Gaussian (LG) beam with $\ell\hbar$ orbital angular momentum (OAM) per photon [9], but any other isolated vortex solutions, e.g., Bessel vortices [19,20] will led to the same results:

$$\Psi_{(f,b)}(z, r, \theta, t) \sim E^0_{(f,b)}\sqrt{2\epsilon_0} \cdot \frac{\exp[-i\omega_{(f,b)}t \pm ik_{(f,b)}z \pm i\ell\theta]}{(1 + iz/z_R)} (r/D_0)^{|\ell|} \exp\left[-\frac{r^2}{{D_0}^2(1 + iz/z_R)}\right], \quad z_R = k_{(f,b)}{D_0}^2, \tag{1}$$

where the cylindrical coordinates (z, r, θ) are used, D_0 is the vortex radius, z_R is the Rayleigh range, Ψ_f and E_f stand for the forward wave, propagating in the positive Z direction, and Ψ_b and E_b stand for the conjugated wave propagating in the opposite direction. Of special interest is the subhertz-order frequency splitting $\delta\omega/2\pi = c(k_f - k_b)/2\pi$, which appears due to the slow mechanical rotation of setup [3,21]. It was already shown that rotation of the $\lambda/2$ wave plate with angular frequency $\Omega \sim 2\pi(1\text{–}100)$ rad/s in one arm of a Mach–Zehnder interferometer induces the rotational Doppler shift (RDS) $\delta\omega = 2\Omega\ell$ for circularly polarized broadband CW with linewidth $\Delta\omega/2\pi \simeq 10^{10}$ Hz. In this configuration, the broadband spectrum was shifted *as a whole* via mechanical rotation (by the angular Doppler effect) at $\delta\omega/2\pi = \pm 2 \cdot 7$ Hz and the beats at the output mirror induced an appropriate rotation of the interference pattern [22].

2. PHASE-CONJUGATING MIRROR IN A REST FRAME

Let us consider first the single-arm phase-conjugating vortex interferometer (PCVI) when the PCM is in the rest frame. Because of the reflection from the PCM, the helical photon with a *linear* polarization proves to be in a superposition of the two counterpropagating quantum states $\Psi_{f,b}$ [Fig. 1]. Currently the best candidate for the *ideal* single-photon PCM is a thick hologram written with sufficiently high diffraction efficiency ($R \sim 0.9$) for the ℓ-charged optical vortex [3,23,24]. In such a case, the amplitudes of the forward and backward fields are close to each other and visibility of the interference pattern $V(\delta L)$ is close to 1, provided that coherence length $L_c \sim 2\pi c/\Delta\omega$ is bigger than the doubled length of the PCVI.

The *ideal* PCM ensures the perfect coincidence of the helical phase surfaces of the counterpropagating optical vortices $\Psi_{f,b}$ and zeros of their electric field amplitudes on the z axis. In contrast to the speckle fields whose interference pattern is composed of intertwined Archimedean screws [25], in a PCVI the isolated Archimedean screw pattern appears both for the *single* photon with an LG wave function and for CW. This results in the intensity profile I_{tw} composed of 2ℓ twisted fringes [7,26,27]:

$$z' = z - z_{pc}, |\Psi|^2 = |\Psi_f + \Psi_b|^2 \sim I_{tw}(z', r, \theta, t)$$
$$= \frac{2\epsilon_0 c|E_{(f,b)}|^2 2^{(|\ell|+1)}(r/D_0)^{2|\ell|}}{\pi\ell! {D_0}^2(1 + z'^2/{z_R}^2)} \cdot \exp\left[-\frac{2r^2}{{D_0}^2(1 + z'^2/{z_R}^2)}\right]$$
$$\times [1 + R^2 + 2R \cdot \cos[\delta\omega \cdot t - (k_f + k_b)z' + 2\ell\theta]], \quad (2)$$

where z_{pc} is the location of the PCM entrance window. Geometrically, the infinitesimal rotation of the Dove prism at the angle $d\theta$ leads to the appropriate phase change of $d\theta \cdot 2\ell$ [28,29]. Thus, the angular speed of pattern rotation $\dot{\theta} = \delta\omega/2\ell$ is given by differentiation of the self-similar argument $2\theta(t) \cdot \ell + \delta\omega \cdot t - (k_f + k_b)z'$ [22] versus time t. Consider the origin of RDS $\delta\omega$ [3,10–12,14] for the photon with topological charge ℓ after the double passage through a Dove prism rotating with angular velocity $\vec{\Omega}$ and reflection from the PCM. OAM projection on the propagation axis is $\langle\Psi_{f,b}|\hat{L}_z|\Psi_{f,b}\rangle = \pm\ell\hbar$, where $\hat{L}_z = -i\hbar \cdot \partial/\partial\theta$.

The RDS occurs because the optical torque on a slowly rotating element changes the angular momentum of the prism

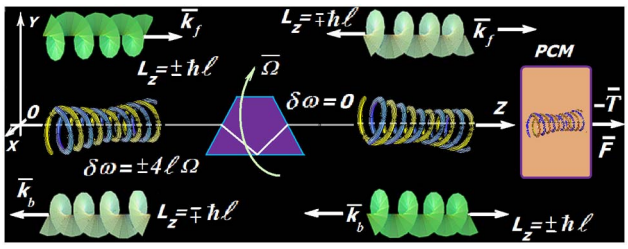

Fig. 1. (Color online) Additivity of RDS for the PCM-reflected photon in the rest frame. Rotation of the Dove prism (positive Ω) decreases frequency to $-2\ell \cdot \Omega$ of the corotating incident photon with $L_z = +\ell\hbar$. Reflection from the helical grating inside the PCM [7,8] alters L_z projection to the opposite one, and counterclockwise rotation of the Dove prism (as seen to backward photon) again decreases the frequency of the corotating photon to $-2\ell \cdot \Omega$. The helical interference pattern is static between the prism and the PCM (where $\delta\omega = 0$) and rotates *before* the prism with angular velocity $\dot{\theta} = -2\Omega$ having *opposite* handedness.

[9,16]. In turn, this changes the prism's angular velocity $\vec{\Omega}$ and such a change requires an energy supply. Because typical optical elements, including prisms, are macroscopic classical objects having a *continuous spectrum* of energies, the energy $\hbar\omega_{f,b}$ and the frequency of the photon may be changed continuously [22].

In the following phase-conjugating optical interferometer, the photon's OAM direction is altered, as well [9,30] (Fig. 1). Let the optical vortex $E_f(t, \vec{r})$ of charge ℓ pass through a rotating Dove prism and to be reflected with $E_b(t, \vec{r})$ from some *ideal* PCM. The nonrotating PCM is supposed to produce *no* frequency shift, as it happens in some cases in photorefractive crystals [7,8], degenerate four-wave mixing [5,30], and holographic PC couplers [3,23]. Note that a small 10^{-1}–10 Hz frequency shift in a $BaTiO_3$ photorefractive PCM may mask the RDS. These additional frequency shifts caused by slow internal charge waves and filamentation effects were reported in the early 1980s [31,32].

Because space is homogeneous and isotropic, the conservation of the momentum and angular momentum is expected [33]. Following [11,22], we have the conservation laws for the projection of the angular momenta L_z on the z axis and the energies of the incident photons and those transmitted through the Dove prism when the latter rotates with the angular velocity $\vec{\Omega}$:

$$I_{zz} \cdot \Omega + L_z = I_{zz} \cdot \Omega' + L'_z\hbar\omega_f + \frac{I_{zz}\Omega^2}{2} = \hbar\omega' + \frac{I_{zz}\Omega'^2}{2}, \quad (3)$$

where I_{zz} is the moment of inertia around the z axis; the left-hand sides of this system correspond to the incident photon and the right-hand sides correspond to the transmitted one. For the incident $L_z = +\ell\hbar$ and passed $L'_z = -\ell\hbar$, Eq .(3) gives the difference of the angular velocities of the prism before and after the photon passage:

$$\Omega - \Omega' = -\frac{2\ell \cdot \hbar}{I_{zz}}. \quad (4)$$

This means that corotation increases the angular velocity of the prism, because the energy is transmitted to the prism by virtue of the optical torque $|\vec{T}| = 2\ell \cdot P/\omega_f$, where P is the total power carried by LG [3] and, hence, Doppler frequency shift for the photon $\omega' - \omega_f$ is negative:

$$\delta\omega = \omega' - \omega_f = \frac{I_{zz}}{2\hbar}(\Omega - \Omega')(\Omega' + \Omega) = -2\ell \cdot \Omega - \frac{2\ell \cdot \hbar}{I_{zz}}. \quad (5)$$

Obviously, in the counterrotating case, when projections of $\vec{\Omega}$ and L_z are in the opposite directions, the rotational Doppler shift is positive. The net RDS during total forward–backward passage is additive due to the PCM and this results in the net OAM change $\delta\omega = \pm 4\ell \cdot \Omega$. The frequency shift $\delta\omega$ is zero between the Dove prism and the PCM and the helical pattern is static there. In the region before the Dove prism, the frequency shift causes the clockwise ($\delta\omega = -4\ell \cdot \Omega$) or counterclockwise ($\delta\omega = +4\ell \cdot \Omega$) rotation of the helix pattern [9] with the angular speed $\dot{\theta} = \pm 2\Omega$ [Eq. (2)].

Because of the angular momentum conservation, the PCM feels the *rotational recoil*, which is proportional to

topological charge ℓ: $|\vec{T}_{pc}| = \ell \cdot P(\omega_f^{-1} + \omega_b^{-1})$, where $P \sim \int_0^\infty |E_{f,b}|^2 r dr$ is the power transferred by the LG beam. The Dove prism feels doubled torque : $|\vec{T}_{\mathrm{Dove}}| = 2\ell \cdot P(\omega_f^{-1} + \omega_b^{-1})$. Note that Lebedev radiation pressure force on the PCM is always directed in the positive Z direction and $|\vec{F}_{pc}| = 2 \cdot P/c$ is independent of ℓ [34].

In the absence of the true PCM when the forward beam is retroreflected by spherical mirror M (Fig. 2) without altering the angular momentum, the interference pattern is a toroidal one I_{tor} [7,9,19,35]:

$$|\Psi|^2 = |\Psi_f + \Psi_b|^2 \sim I_{\mathrm{tor}}(z', r, \theta, t) = \frac{2\epsilon_0 c |E_{(f,b)}|^2 2^{(|\ell|+1)} (r/D_0)^{2|\ell|}}{\pi \ell! D_0{}^2 (1 + z'^2/z_R{}^2)} \cdot \exp\left[-\frac{2r^2}{D_0{}^2(1 + z'^2/z_R{}^2)}\right][1 + R^2 + 2R \cdot \cos[\delta\omega \cdot t - (k_f + k_b)z']]. \quad (6)$$

The RDS is not accumulated here (the Doppler shifts for the forward and backward photons cancel each other $\delta\omega = 0$) because true PC is absent; hence, the toroidal interference pattern is static. The mechanical torques on prism $\vec{T}$ induced by OAM alternation will cancel each other, too: $|\vec{T}| = 2\ell \cdot P(\omega_f^{-1} - \omega_b^{-1}) \cong 0$.

3. PHASE-CONJUGATING MIRROR IN A ROTATING FRAME

The more fundamental case is a rotation of the setup as a whole around some axis and this general case is relevant to the detection of the slow rotations of the reference frame [1]. In contrast to a Sagnac interferometer, where the frequency splitting and running interference pattern appear in the active loop only, the PCVI produces frequency splitting $\delta\omega$ without optical gain (Fig. 3). Apparently, the RDS $\delta\omega$ will be the same when a CW laser source is placed in both the inertial (rest) frame and in the noninertial frame associated with the rotating vehicle. For the simplest case, when the sole PCM rotates around propagation axis z of a twisted photon with charge ℓ, the RDS appears due to the alternation of the photon's OAM. Again Eqs. (3) give the frequency shift $\delta\omega = \omega_b - \omega_f$ due to the reflection from the rotating PCM:

$$\delta\omega = \omega_b - \omega_f = \pm 2\ell \cdot \Omega + \frac{2\ell \cdot \hbar}{(I_{zz})_{\mathrm{PCM}}}. \quad (7)$$

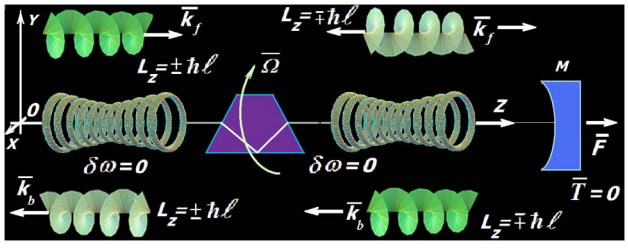

Fig. 2. (Color online) Mutual cancellation of RDS for a retroreflected photon. Rotation of the Dove prism again decreases frequency of the corotating forward photon with $L_z = +\ell\hbar$ by $-2\ell \cdot \Omega$. In backward propagation, the Dove prism is counterrotating with respect to the photon. Backward RDS is positive; thus, the resulting $\delta\omega$ is zero and the toroidal interference pattern is static for all Z.

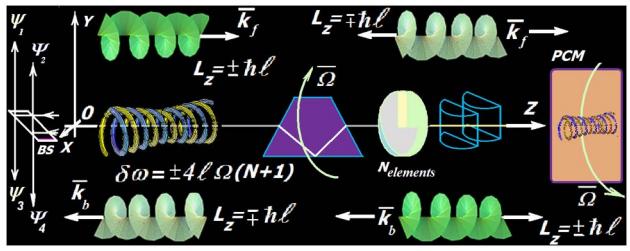

Fig. 3. (Color online) Additivity of RDS in PCVI inside the rotating vehicle. The sign of $\delta\omega$ is positive when optical torque $\vec{T}$ produced by a bunch of the rotating photons upon the mirror has the opposite direction compared to the rotation frequency of the PCM $\vec{\Omega}$. When the Dove prism rotates in the opposite direction versus the PCM, the net RDS reaches the sixfold value $\delta\omega = \pm 6\ell \cdot \Omega$ due to the additional OAM alternation. The sequence of N counterrotating OAM-altering elements (including helical wave plates and cylindrical lenses) will produce net RDS of $\delta\omega = 4\ell \cdot \Omega(N + 1/2)$ value. $|\Psi_{1,2,3,4}\rangle$ designates the antibunching of photons, which belongs to the *two* (for $\ell = 1$) helical wave functions, separated by a $\lambda/2$ interval, deflected by the entrance beam splitter [7].

The second term in the right-hand side of Eq. (7) is negligible for typical masses ($m \sim$ g) and sizes ($r \sim$ cm) of prisms and mirrors $\hbar/I_{zz} \sim \hbar/(m \cdot r^2) \cong 10^{-27}$ Hz, as in Beth's [16] and Dholakia and co-worker's [22] experiments for the interaction of circularly polarized photons with a macroscopic object (half-wavelength plate).

The angular speed of rotation of the interference pattern proves to be $\dot{\theta} = \delta\omega/2\ell = \Omega$; thus, the pattern rotates synchronously with the reference frame. The helical interference pattern outside the PCM will be dragged by the helical diffraction grating [9] within the PCM. Consequently, the sole PCM cannot detect frame rotation. Note that conventional photorefractive [7,8] or static holography mechanisms [24] are sufficient to observe this drag effect and the atomic coherence is not necessary in our case, as compared to [36].

Nevertheless, there exists a possibility to accumulate the RDS by means of a chain of OAM-alternating elements. To achieve the accumulation of RDS, the adjacent components of the PCVI must rotate in opposite directions $\vec{\Omega}_n = (-1)^n\vec{\Omega}$, where $n = 0$ stands for the PCM, $n = 1$ for the Dove prism adjacent to the PCM, and $n = N$ for the last Dove prism near the beam splitter. This is necessary because OAM is altered after the passage of each Dove prism and the mutual orientation of the angular momenta of the photon and the next prism should be maintained throughout the chain. When *even* elements (the PCM itself and $N/2$ Dove prisms) of the PCVI are fixed in the $\vec{\Omega}$ rotating frame, the other $N/2$ *odd* elements ought to rotate with the *bias* angular velocity $-2\vec{\Omega}$. The chain of the N rotating OAM-alternating elements will produce the net rotational Doppler shift amounting to $\delta\omega = 4\ell \cdot \Omega(N + 1/2)$. Thus, the PCVI interference pattern (Fig. 3) will revolve with enhanced angular speed $\dot{\theta} = \pm 2 \cdot (N + 1/2) \cdot \Omega$.

In such a way, the PCVI (Fig. 3) may be used for demonstration of the possibility of detection of the sub-Hertzian rotation of the reference frame with the Earth ($\Omega_\oplus \sim 2\pi/86{,}400$). The helical interference pattern will rotate much faster than Earth itself. Namely, the equation $4\ell \cdot (N + 1/2) = 24$ has only one solution for integer ℓ, N ($\ell = 4$, $N = 1$). Hence, the optical vortex with charge $\ell = 4$ passed twice through the single Dove prism rotating with $\vec{\Omega}_\oplus$ and

the PCM rotating in the opposite direction $-\vec{\Omega}_{\oplus}$ will produce at the entrance beam splitter BS the $2\cdot\ell$ spots of the interference pattern revolving once per hour.

The further accumulation of RDS in the PCVI might be achieved by means of installing the $N=60$ counterrotating image-inverting elements and $\ell=6$ optical vortex. In such configuration, the $2\cdot\ell$ helices of the interference pattern [Eq. (2)] will produce 2ℓ spots at the PCVI beam splitter with one pass through the detector window within approximately each 60 s. For this purpose, the even components (the PCM and $N/2$ Dove prisms) may be fixed at setup to rotate with velocity $\vec{\Omega}_{\oplus}$, while the other $N/2$ prism should rotate with bias angular velocity $-2\vec{\Omega}_{\oplus}$ with respect to the rotating setup (e.g., rotating table). This enhancement will model the detection of the Earth's rotation, and this will alter the $\ell\hbar$ OAM of *each* photon 121 times during one passage through the PCVI. Apart from the Dove prisms, the other OAM-altering helical wave plates and cylindrical lenses may be used [11,15,23]. The required helical interference pattern within the PCVI might also be written by means of atomic coherence effects in a solid-state resonant medium [36]. Note that, in the proposed measurement of the Earth's rotation, $\delta\omega=\pm 4\ell\cdot(N+1/2)\Omega_{\oplus}\cos(\phi)$ will show dependence on geographical latitude ϕ as it is known for the Foucault pendulum [37]: on the poles, $\delta\omega$ will be equal to the maximum value when the angle ϕ between normal and the PCVI axis is 0 or π, while at the equator, $\delta\omega$ might reach the maximum value when the PCVI axis is parallel to Earth's rotation axis. The preliminary analysis has shown that the laser linewidth of the order $\Delta\omega/2\pi\sim 10^3$ Hz might be sufficient for Earth rotation detection by the PCVI (Fig. 3).

4. SINGLE-PHOTON OPERATION OF THE PHASE-CONJUGATING VORTEX INTERFEROMETER

Single-photon operation [18] is based upon the superposition of the forward and backward quantum states with $\ell\hbar$ OAM:

$$|\Psi\rangle_H=\frac{1}{\sqrt{2}}(|\Psi_{\pm\ell\hbar}\rangle_f+|\Psi_{\mp\ell\hbar}\rangle_b)=\frac{1}{\sqrt{2\ell}}\sum_{j_h}|\Psi_{j_h}\rangle. \quad (8)$$

The detection of this superposition is not a trivial two-detector procedure, because the interference pattern is composed of 2ℓ twisted helices $|\Psi_{j_h}\rangle$. The entrance beam splitter will reflect both upward and downward the interference pattern [7,9] composed of the 2ℓ spots located on an ellipse, rather than independent forward $|\Psi_{\pm\ell\hbar}\rangle_f$ and backward $|\Psi_{\mp\ell\hbar}\rangle_b$ photon states. For the simplest case $\ell=1$, the photon will be in the superpositional state of the two *helical* wave functions designated by appropriate colors at Fig. 3:

$$|\Psi\rangle_H=\frac{1}{\sqrt{2}}(|\Psi_{\mathrm{Blue}}\rangle+|\Psi_{\mathrm{Yellow}}\rangle). \quad (9)$$

This means that two detectors (for $|\Psi_1\rangle$ and $|\Psi_2\rangle$) placed above the entrance beam splitter [7] and two detectors located below the beam splitter (for $|\Psi_3\rangle$ and $|\Psi_4\rangle$) can indicate the *antibunching* of the photons [1,18], belonging to either of the two helices composing the interference pattern. As in a double-slit Young interference experiment, the attempt of the eavesdropping [1] the *which way* photon moves (the forward or backward one) will reduce the visibility of the helical interference pattern. On the other hand, when the single-photon quantum state is prepared as a toroidal pattern (Fig. 2), the photon belongs to the sequence of the equidistantly spaced toroidal Wannier wave functions $|\Psi_{j_{\mathrm{tor}}}\rangle$ spaced by $\lambda/2$ intervals:

$$|\Psi\rangle_{\mathrm{tor}}=\frac{1}{\sqrt{2}}(|\Psi_{\pm\ell\hbar}\rangle_f+|\Psi_{\pm\ell\hbar}\rangle_b)=\frac{1}{\sqrt{N_{\mathrm{tor}}}}\sum_{j_{\mathrm{tor}}}\Psi_{j_{\mathrm{tor}}}. \quad (10)$$

5. CONCLUSION

In summary, we analyzed the PCVI for the single-photon [18] and CW laser output [7,9]. Because of the alignment of all the optical components along the photon propagation axis z, the PCVI looks promising from the point of view of rotation sensing [1]. The self-adjusting property of the PCM [6] (also referred to as *time reversal*) will provide the automatic compensation of the beam displacements caused by rotations of Dove prisms [3] or rotating lenses [11]. This property is the advantage of the PCVI compared to a Mach–Zehnder interferometer with rotating birefringent $\lambda/2$ plates [22], where additivity of RDS [14] due to the sequence of *spin* angular momentum alternations is also feasible when a sequence of the $\lambda/2$ plates rotates in the opposite directions, as in Fig. 3.

In the PCVI, the accumulation of RDS $\delta\omega$ will enhance the frame rotation $\vec{\Omega}$ by a factor of an even multiple of the photon's topological charge ℓ and of the number of angular-momentum-inverting elements N in the PCVI chain. We hope to consider the above issues, including entanglement of the helical photons [28] in the PCVI due to the mixing of counterpropagating photon vortex states at the beam splitter [38], in more detail in subsequent work.

REFERENCES

1. M. O. Scully and M. S. Zubairy, *Quantum Optics* (Cambridge University, 1997), Chap. 4.
2. J. Leach, M. J. Padgett, S. M. Barnett, S. Franke-Arnold, and J. Courtial, "Measuring the orbital angular momentum of a single photon," Phys. Rev. Lett. **88**, 257901 (2002).
3. A. Bekshaev, M. Soskin, and M. Vasnetsov, *Paraxial Light Beams with Angular Momentum* (Nova Science, 2008).
4. R. W. Boyd, *Nonlinear Optics* (Academic, 2003).
5. B. Y. Zeldovich, N. F. Pilipetsky, and V. V. Shkunov, *Principles of Phase Conjugation* (Springer-Verlag, 1985).
6. N. G. Basov, I. G. Zubarev, A. B. Mironov, S. I. Mikhailov, and A. Y. Okulov, "Laser interferometer with wavefront reversing mirrors," J. Exp. Theor. Phys. **52**, 847–851 (1980).
7. M. Woerdemann, C. Alpmann, and C. Denz, "Self-pumped phase conjugation of light beams carrying orbital angular momentum," Opt. Express **17**, 22791 (2009).
8. A. V. Mamaev, M. Saffman, and A. A. Zozulya, "Time dependent evolution of an optical vortex in photorefractive media," Phys. Rev. A **56**, R1713 (1997).
9. A. Yu Okulov, "Angular momentum of photons and phase conjugation," J. Phys. B **41**, 101001 (2008).
10. B. A. Garetz, "Angular Doppler effect," J. Opt. Soc. Am. **71**, 609–611 (1981).
11. G. Nienhuis, "Doppler effect induced by rotating lenses," Opt. Commun. **132**, 8–14 (1996).
12. I. Bialynicki-Birula and Z. Bialynicka-Birula, "Rotational frequency shift," Phys. Rev. Lett. **78**, 2539–2542 (1997).
13. J. Courtial, D. A. Robertson, K. Dholakia, L. Allen, and M. J. Padgett, "Measurement of the rotational frequency shift imparted to a rotating light beam possessing orbital angular momentum," Phys. Rev. Lett. **80**, 3217–3219 (1998).

14. J. Courtial, D. A. Robertson, K. Dholakia, L. Allen, and M. J. Padgett, "Rotational frequency shift of a light beam," Phys. Rev. Lett. **81**, 4828–4830 (1998).
15. L. Allen, M. W. Beijersbergen, R. J. C. Spreeuw, and J. P. Woerdman, "Orbital angular momentum of light and the transformation of Laguerre-Gaussian laser modes," Phys. Rev. A **45**, 8185–8189 (1992).
16. R. A. Beth, "Mechanical detection and measurement of the angular momentum of light," Phys. Rev. **50**, 115–125 (1936).
17. J. E. Sipe, "Photon wave functions," Phys. Rev. A **52**, 1875–1883 (1995).
18. M. Baier, S. Watanabe, E. Pelucchi, E. Kapon, S. Varoutsis, M. Gallart, I. Robert-Philip, and I. Abram, "Single-photon emission from site-controlled pyramidal quantum dots," Appl. Phys. Lett. **84**, 648–650 (2004).
19. K. Volke-Sepulveda and R. Jauregui, "All-optical 3D atomic loops generated with Bessel light fields," J. Phys. B **42**, 085303 (2009).
20. J. Durnin, J. J. Miceli Jr., and J. H. Eberly, "Diffraction-free beams," Phys. Rev. Lett. **58**, 1499 (1987).
21. M. P. MacDonald, K. Volke-Sepulveda, L. Paterson, J. Arlt, W. Sibbett, and K. Dholakia, "Revolving interference patterns for the rotation of optically trapped particles," Opt. Commun. **201**, 21–28 (2002).
22. J. Arlt, M. MacDonald, L. Paterson, W. Sibbett, K. Volke-Sepulveda, and K. Dholakia, "Moving interference patterns created using the angular Doppler-effect," Opt. Express **10**, 844–852 (2002).
23. E. Abramochkin and V. Volostnikov, "Spiral light beams," Phys. Usp. **47**, 1177–1203 (2004).
24. Ch. V. Felde and P. V. Polyanski, "Static holographic phase conjugation of vortex beams," Opt. Spectrosc. **98**, 913–918 (2005).
25. A. Yu. Okulov, "Twisted speckle entities inside wavefront reversal mirrors," Phys. Rev. A **80**, 163907 (2009).
26. M. Bhattacharya, "Lattice with a twist: helical waveguides for ultracold matter," Opt. Commun. **279**, 219–222 (2007).
27. A. Yu. Okulov, "Phase-conjugation of the isolated optical vortex using a flat surfaces," J. Opt. Soc. Am. B **27**, 2424–2427 (2010).
28. H. Q. Wei, X. Xue, J. Leach, M. J. Padgett, S. M. Barnett, S. Franke-Arnold, E. Yao, and J. Courtial, "Simplified measurement of the orbital angular momentum of single photons," Opt. Commun. **223**, 117–122 (2003).
29. M. P. J. Lavery, A. Dudley, A. Forbes, J. Courtial1, and M. J. Padgett, "Robust interferometer for the routing of light beams carrying orbital angular momentum," New J. Phys. **13**, 093014 (2011).
30. D. M. Pepper, "Phase conjugate optics," Ph.D. dissertation (California Institute of Technology, 1980), p. 37. http://resolver.caltech.edu/CaltechETD-10122006-081036.
31. A. V. Nowak, T. R. Moore, and R. A. Fisher, "Observations of internal beam production in barium titanate phase conjugators," J. Opt. Soc. Am. B **5**, 1864–1878 (1988).
32. S. Sternklar, S. Weiss, and B. Fischer, "Tunable frequency shift of photorefractive oscillators," Opt. Lett. **11**, 165–167 (1986).
33. E. M. Lifshitz, L. P. Pitaevskii, and V. B. Berestetskii, *Quantum Electrodynamics* (Butterworth, 1982), Sections 6 and 8.
34. P. N. Lebedev, "Experimental examination of the light pressure," Ann. Phys. **6**, 433–459 (1901).
35. T. Puppe, I. Schuster, A. Grothe, A. Kubanek, K. Murr, P. W. H. Pinkse, and G. Rempe, "Trapping and observing single atoms in a blue-detuned intracavity dipole trap," Phys. Rev. Lett. **99**, 013002 (2007).
36. S. Franke-Arnold, G. Gibson, R. W. Boyd, and M. J. Padgett, "Rotary photon drag enhanced by a slow-light medium," Science **333**, 65–67 (2011).
37. L. Foucault, "Démonstration physique du mouvent de rotation de la Terre, au moyen d'un pendule," C. R. Hebd. Seances Acad. Sci., **35**, 135–138 (1851).
38. M. Shirasaki, H. A. Haus, and D. L. Wong, "Quantum theory of the nonlinear interferometer," J. Opt. Soc. Am. B **6**, 82–88 (1989).